# Biodegradable Compatibilized Poly(L-lactide) / Thermoplastic Polyurethane Blends: Design, Preparation and Property Testing

**Kanyarat Suthapakti[1] • Robert Molloy[1,2] • Winita Punyodom[1,2] • Kanarat Nalampang[1] • Thanawadee Leejarkpai[3] • Paul D. Topham[4] • Brian J. Tighe[5]**

[1] Polymer Research Group, Department of Chemistry, Faculty of Science, Chiang Mai University, Chiang Mai 50200, Thailand

[2] Materials Science Research Center, Faculty of Science, Chiang Mai University, Chiang Mai 50200, Thailand

[3] National Metal and Materials Technology Center, National Science and Technology Development Agency, Thailand Science Park, Pathum Thani 12120, Thailand

[4] Aston Institute of Materials Research, Aston University, Birmingham B4 7ET, UK

[5] Department of Chemical Engineering and Applied Chemistry, School of Engineering and Applied Science, Aston University, Birmingham B4 7ET, UK

✉ Robert Molloy; robert.m@cmu.ac.th

## Abstract

Biodegradable blends of poly(L-lactide) (PLL) toughened with a polycaprolactone-based thermoplastic polyurethane (TPU) elastomer and compatibilized with a purpose-designed poly(L-lactide-*co*-caprolactone) (PLLCL) copolymer were prepared. Both 2-component (PLL/TPU) and 3-component (PLL/TPU/PLLCL) blends of various compositions were prepared by melt mixing, hot-pressed into thin films and their properties tested. The results showed that, although the TPU could toughen the PLL, the blends were immiscible leading to phase separation with the TPU domains distributed in the PLL matrix. However, addition of the PLLCL copolymer could partially compatibilize the blend by improving the interfacial adhesion between the two phases. Biodegradability testing showed that the blends were biodegradable and that the PLLCL copolymer could increase the rate of biodegradation under controlled composting conditions. The 3-component blend of composition PLL/TPU/PLLCL = 90/10/10 parts by weight was found to exhibit the best all-round properties.

**Keywords :** Poly(L-lactide) • Thermoplastic polyurethane elastomer • Poly(L-lactide-*co*-caprolactone • Immiscible blend • Compatibilization • Biodegradability

## Introduction

Biodegradable plastics are plastics that decompose naturally in the environment. This is achieved when microorganisms present in the environment metabolize and break down the polymer structure, usually in combination with other degradative factors such as temperature, light, moisture and oxygen. When this biodegradation occurs in soil, the plastic is also said to be compostable and there are now several procedures for following aerobic biodegradation under controlled composting conditions such that described in the recent ASTM D5338-15 Standard Test Method [1].

Among the family of biodegradable polyesters, poly(L-lactide) (PLL), or poly(lactic acid) (PLA) as it is more commonly referred to in the bioplastics industry, has been the focus of much attention since it is produced from renewable resources, shows good transparency in the form of film, cups and bottles, exhibits mechanical properties comparable to those of many commercial polymers, and is processable using conventional thermoplastic processing equipment. Its rise to prominence in recent years has been well documented and there is now a vast library of information available on PLL in both books and journals [2-8].

However, PLL also has some notable disadvantages such as its low heat deflection temperature of around 60 ºC, brittleness in certain applications, slow rate of crystallization, and inferior water vapor and gas barrier properties. Consequently, in order to diversify PLL's range of applications, there is increasing interest nowadays in how its properties can be modified by, for example, (1) the use of additives such as nucleating agents, plasticizers and impact modifiers, (2) blending with other polymers, and (3) nanocomposites with inorganic materials such as clay, zinc oxide, titanium dioxide and carbon nanotubes. Of these three approaches, blending with other polymers has received the most attention and it is this approach which has been employed in the work described in this paper.

Although PLL has been blended with a wide range of different polymers, blending has mainly been with other aliphatic polyesters or with polymers containing substituent ester groups in the expectation that the polar interactions between the ester groups would aid miscibility. Examples include PLL blends with polycaprolactone (PCL) [9-11], polyhydroxybutyrate (PHB) [12], poly(butylene succinate) (PBS) [13,14], poly(butylene adipate-*co*-terephthalate) (PBAT) [15], cellulose acetate butyrate (CAB) [16] and ethylene-*co*-vinyl acetate (EVA) [17]. However, despite the ester group interactions, these blends have been shown to be largely immiscible over a wide range of composition and have so far found very limited application.

Regarding PLL's blends with other types of polymers, perhaps the most interesting has been its blends with thermoplastic polyurethane (TPU) elastomers [18-25]. Even though results have shown that PLL and TPU are also largely immiscible with the TPU distributed as discrete domains in the PLL matrix, the fact that TPU can toughen PLL to some extent, increase its elongation at break, and transform its brittle fracture into a more ductile fracture is an indication of at least some interfacial interaction. This interaction is thought to occur mainly through hydrogen bonding (–C=O···H–N–) between the ester groups in PLL and the urethane groups in TPU [18].

This paper now describes the melt blending of PLL with a polycaprolactone-based (PCL-based) TPU elastomer. Even though PCL has been shown to be partially miscible with PLL in PLL/PCL blends [9-11], the presence of PCL soft segments in a PCL-based TPU does not appear to significantly improve the interfacial adhesion in PLL/TPU blends. Therefore, the challenge and also the novel aspect of this work has been to introduce a purpose-designed third component which can act as a compatibilizer to increase the level of interaction and therefore the interfacial adhesion between the PLL matrix and the TPU domains. This third component is a medium molecular weight, amorphous poly(L-lactide-*co*-caprolactone)50:50

copolymer, PLLCL, which through its LL and CL contents can act as a "bridge" between the PLL and the PCL-based TPU. The main target application for this 3-component blend is biodegradable film packaging but clearly other applications based on injection molded parts and extruded fibers are also possible.

## Materials and Methods

### Commercial Materials

The PLL used was a commercial product, Ingeo™ 4042D Film Grade PLA (NatureWorks®), in pellet form. As received, the PLL had number-average and weight-average molecular weights, $M_n$ and $M_w$, of 1.52 x $10^5$ and 2.55 x $10^5$ g/mol respectively, as determined by gel permeation chromatography (GPC).

The polycaprolactone-based thermoplastic polyurethane (TPU) elastomer used was also a commercial product, Pellethane™ 2102-75A (Lubrizol Corporation), in pellet form where 75A denoted the Shore hardness. Its structure consisted of alternating hard and soft segments based on 4,4'-methylene diphenyl diisocyanate (MDI) and polycaprolactone diol respectively together with 1,4-butanediol (BDO) as a chain extender. The TPU elastomer had $M_n$ and $M_w$ values of 1.28 x $10^5$ and 2.62 x $10^5$ g/mol respectively from GPC. In addition, two other Pellethane™ grades were also studied for comparison, namely 2102-80A and 2102-90A. However, the 2102-75A grade was found to be the most suitable for melt blending with the PLL due to its lower melt viscosity and lower initial melt flow temperature (≈ 175 °C).

### Copolymer Synthesis

L-Lactide (LL) monomer was synthesized from L-lactic acid (Grand Chemical Far East Ltd., 88 %) by well-established procedures and purified by repeated recrystallization from ethyl acetate [26]. After drying to constant weight in a vacuum oven at 50 °C for 24 h, pure LL was obtained as a white, needle-like crystalline solid with a chemical purity of ≥ 99.5 % (from DSC purity analysis). ε-Caprolactone (CL) monomer (Acros, 99 %) was purified by vacuum distillation over calcium hydride (b.pt. 60 °C/2-3 mmHg). Tin(II) octoate, $Sn(Oct)_2$, initiator (Sigma-Aldrich, 95 %) was purified by heating at 120 °C with stirring under vacuum in order to remove the octanoic acid and moisture impurities.

The poly(L-lactide-*co*-caprolactone) copolymer, PLLCL (LL:CL = 50:50 mol%), was synthesized by ring-opening copolymerization in bulk of equimolar amounts of LL and CL monomers at 120 ºC for 72 h with 0.1 mol% $Sn(Oct)_2$ as the initiator. The crude copolymer product was purified by cutting into small pieces and heating under vacuum at 40 ºC for 24 h to constant weight to remove any residual monomers. The final purified product, which was purposely synthesized to only a medium molecular weight, had $M_n$ and $M_w$ values of 2.43 x $10^4$ and 4.40 x $10^4$ g/mol respectively from GPC and was obtained in approximately 95 % yield. The chemical structure of the PLLCL copolymer is compared with those of PLL and TPU in Fig. 1.

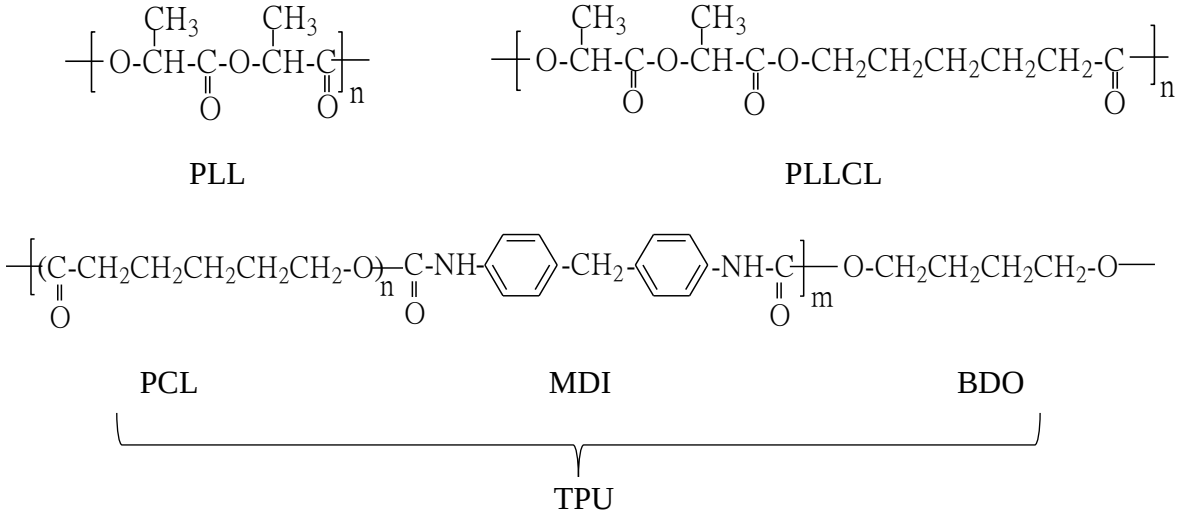


**Fig. 1** Chemical structures of the PLL, PLLCL and TPU blend components

## Polymer Blending and Film Preparation

Polymer blending was carried out by means of melt mixing using a Haake Polylab Internal Mixer at a temperature of 195 ºC for the PLL/TPU 2-component blends and 190 ºC for the PLL/TPU/PLLCL 3-component blends for 20 min. These were the lowest temperatures and shortest time necessary to ensure complete melting and homogeneous mixing while at the same time minimizing the extent to which thermal degradation of the PLL might occur. Prior to melt mixing, the polymer pellets were each rigorously pre-dried in a vacuum oven at 40 ºC for 12 h and then pre-mixed in their dry state before storing in a vacuum desiccator. As a further precaution, the mixing chamber of the internal mixer was deaerated and dehumidified as much as possible by flushing with dry nitrogen gas. Subsequent GPC measurements confirmed that, even at the higher processing temperature of 195 °C, molecular weight reduction of the PLL due to thermal degradation was less than 20 %. After the melt blends had been ground into small pieces, thin films of thickness 150-200 μm were prepared using a LabTech Engineering LP-S-20 Laboratory Press at a temperature of 180 ºC and 20 MPa pressure for 5 min. Following their preparation, the films were stored in a desiccator before testing.

## Instrumental Methods

Copolymer composition and microstructural analysis were carried out using a Bruker Avance DRX-400 Nuclear Magnetic Resonance Spectrometer operating at field frequencies of 400 MHz for $^{1}$H-NMR and 100 MHz for $^{13}$C-NMR. Deuterated chloroform ($CDCl_3$) was used as the solvent with tetramethylsilane (TMS) as the internal standard.

Polymer molecular weight determination was performed using a Varian PL-GPC 50 Plus Gel Permeation Chromatograph (tetrahydrofuran solvent, 40 °C, flow-rate 1 ml/min)

equipped with a refractive index detector and calibrated with narrow molecular weight distribution polystyrene standards.

Thermal analysis for determining the glass, crystallization and melting transition temperatures ($T_g$, $T_c$, $T_m$) and initial thermal decomposition temperature ($T_d$) were carried out using a Perkin-Elmer DSC7 Differential Scanning Calorimeter (-50→200 °C, heating rate 10 °C/min) and a Perkin-Elmer TGA7 Thermogravimetric Analyzer (50→550 °C, heating rate 20 °C/min) respectively.

Where DSC was unable to detect the $T_g$ clearly, such as for the TPU, a Mettler-Toledo DMA/STDA861e Dynamic Mechanical Analyzer was employed instead (-80→80 °C, heating rate 4 °C/min, oscillation frequency 1 Hz, tension mode).

Melt flow index (*MFI*) measurements were carried out using a Lloyd Instruments MFI-10 Melt Flow Indexer at 190 °C (load 2.16 kg, bore diameter 2.1 mm) in accordance with the ASTM D1238-13 test method for melt flow rates of thermoplastics [27].

Tensile testing of thin films was performed using a Lloyds LRX+ Universal Testing Machine in accordance with the ASTM D882-02 test method for thin plastic sheeting [28]. Test specimens were conditioned at 23±2 °C and 50±5 % relative humidity for 48 h prior to testing. At least 5 specimens were tested for each sample (gauge length 100 mm, crosshead speed 50 mm/min).

For microscopic analysis of tensile fracture surfaces, specimens were mounted on stainless steel stubs with a conductive carbon tape, gold-coated and then imaged using a JEOL JSM 5910LV Scanning Electron Microscope (SEM) operating with an accelerating voltage of 15 kV at 23 °C.

Percent light transmittance (*%T*) of thin films as a measure of optical clarity was measured using a Molecular Devices SpectraMax® M2 UV-Visible Multimode Microplate

Reader at a wavelength of 450 nm with air as the reference. Measurements were taken from at least 5 different areas of the film and averaged.

Water vapor transmission rate (*WVTR*) measurements were made using a Systech Illinois 7002 Water Vapor Permeation Analyzer in accordance with the ASTM F1249-13 test method for *WVTR* through plastic film and sheeting [29]. Measurements were made on film samples over a circular surface area of 50 $cm^2$ at 37.8 °C and 90 % relative humidity.

Oxygen permeability, as expressed in terms of the oxygen transmission rate (*OTR*), was measured using a PERME® VAC-V1 Gas Permeability Tester according to the ASTM D3985-05 test method for *OTR* through plastic film and sheeting [30]. Test specimens were cut into 10 cm x 10 cm squares and clamped on the oxygen diffusion chamber of diameter 8 cm at 23 °C and with a gas pressure of 1.00 $kg.f/cm^2$.

## Biodegradability Testing

Biodegradability testing was performed according to the ISO 14855-1:2005 standard test procedure for determining the ultimate aerobic biodegradability of plastic materials under controlled composting conditions [31]. Test samples were ground to a particle size < 500 μm and compared with microcrystalline cellulose of particle size 20 μm as a reference material. Biodegradation was carried out in well-aerated compost with a constant moisture content of 50-55 % at 58 ± 2 °C for 90 days in 2-liter glass vessels. Biodegradation was followed by continuously measuring the amount of $CO_2$ evolved in the exhaust air as dissolved inorganic carbon (DIC) after absorption in sodium hydroxide solution. The % biodegradation was then calculated by comparing the amount of $CO_2$ evolved with the maximum theoretical amount of $CO_2$ calculated from the test material's total organic carbon content. The test system was set up as shown in Fig. 2.

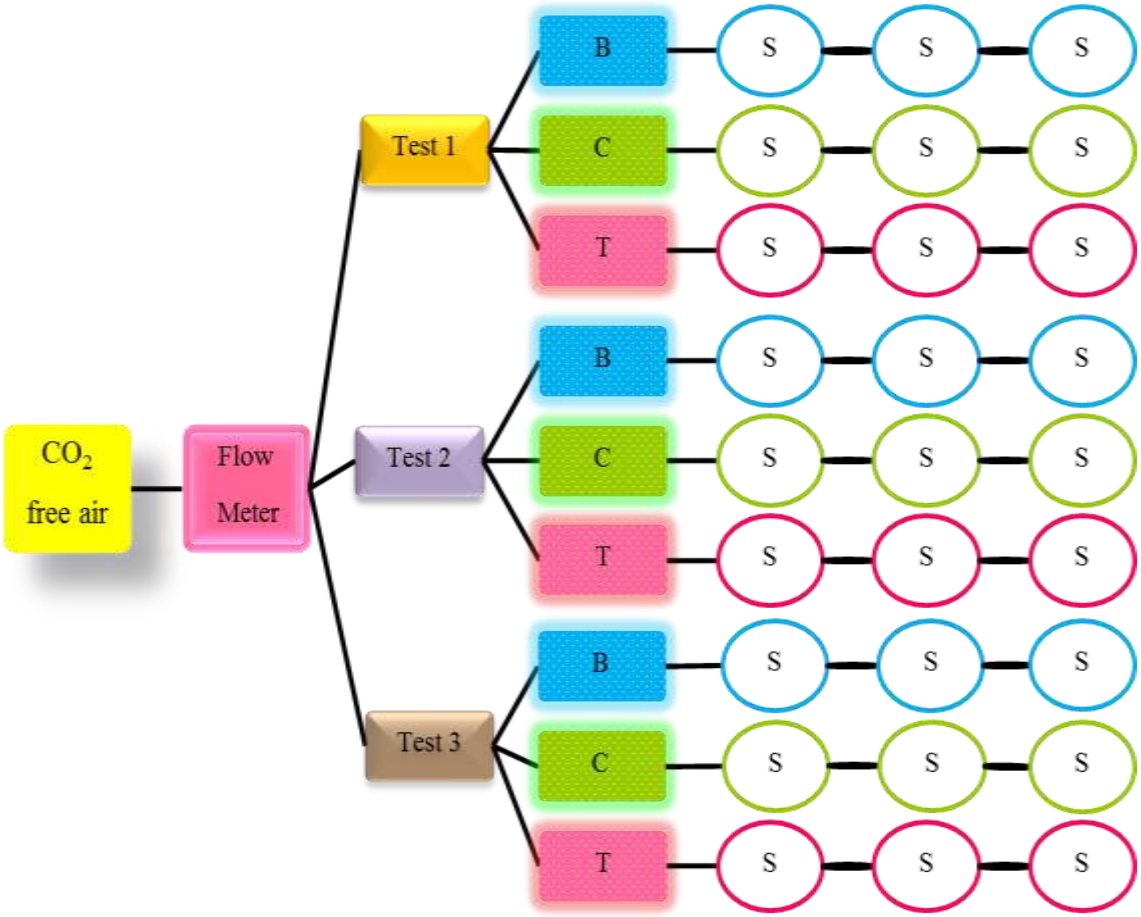


**Fig. 2** Schematic diagram of the biodegradability test system.
B = blank, C = cellulose reference, T = test sample, S = scrubbing solution (NaOH)

## Results and Discussion

### Copolymer Characterization

The PLLCL copolymer was obtained as a colorless, translucent, rubbery solid. From its $^{1}$H-NMR spectrum in Fig. 3, its composition could be calculated from the peak area integrations of the LL methine protons (b) at $\delta$ 5.1-5.3 and the CL ε-methylene protons (c) at $\delta$ 4.0-4.2. Since the copolymer was obtained in near-quantitative yield (≈ 95 %), its composition of LL:CL = 51:49 (mol%) was very similar to the initial equimolar (50:50) comonomer feed.

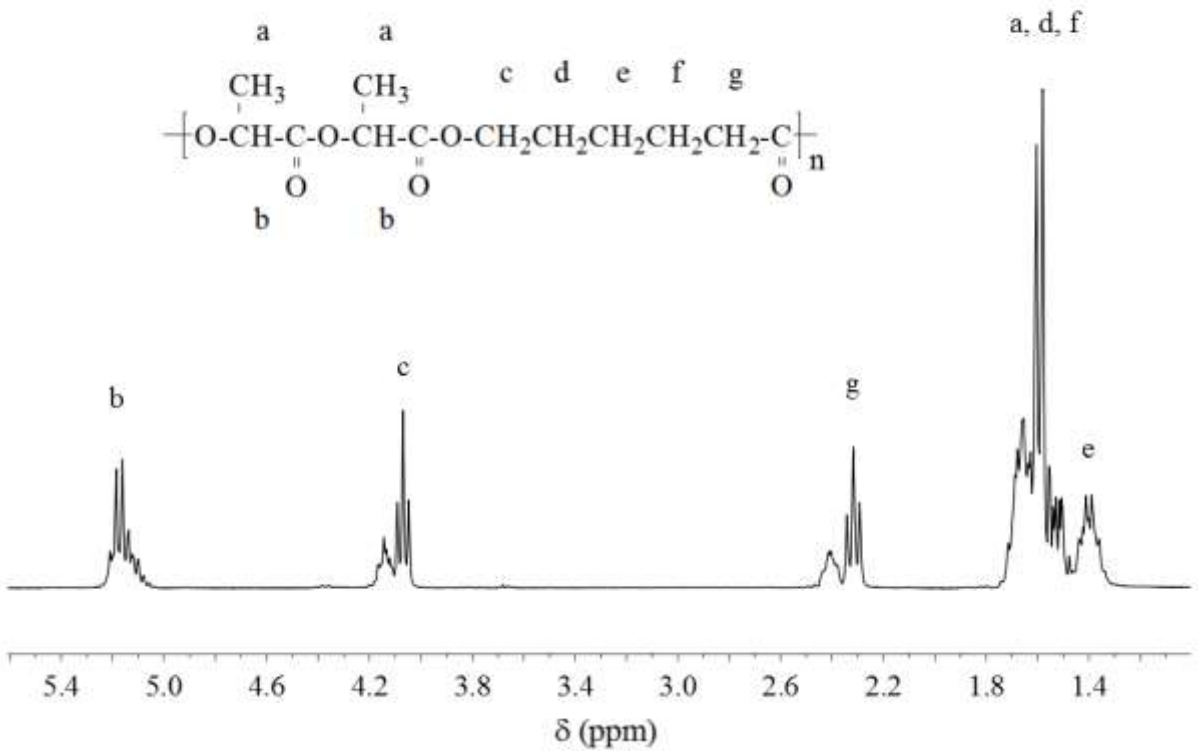


**Fig. 3** 400 MHz $^{1}$H-NMR spectrum of the PLLCL 50:50 copolymer recorded in $CDCl_3$ as solvent.

More detailed microstructural information regarding the copolymer's monomer sequencing could be obtained from its $^{13}$C-NMR spectrum, specifically from the expanded carbonyl carbon (C=O) region from $\delta$ = 169-174 ppm, as shown in Fig. 4. The heterotriad peaks in between the CCC and LLL homotriad peaks are a measure of the degree of randomness of the monomer sequencing. In the triad notations in Fig. 4, C represents a CL unit while L represents an LL half-unit. For example, the LCL triad sequence corresponds to:

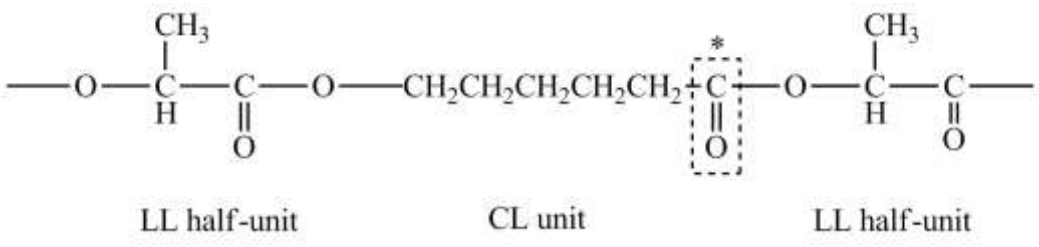

and its peak in the spectrum is that of the central carbonyl carbon (*). The fact that the LLL and CCC peaks are so much more prominent than the rest is an indication that the monomer sequencing is tapered (i.e., partly blocky) rather than purely random. This is a consequence of the much different monomer reactivity ratios ($r_{LL} >> r_{CL}$). Earlier work reported reactivity ratios of $r_{LL}$ = 34.7 and $r_{CL}$ = 0.24 for the LL-CL bulk copolymerization at 130 ºC using $Sn(Oct)_2$ as the initiator [32]. However, in practice, this tapered monomer sequencing is randomized to a certain extent by the transesterification reactions which occur in the melt during synthesis. Monomer sequencing in PLLCL copolymers has been studied extensively by $^{13}$C-NMR [33-36].

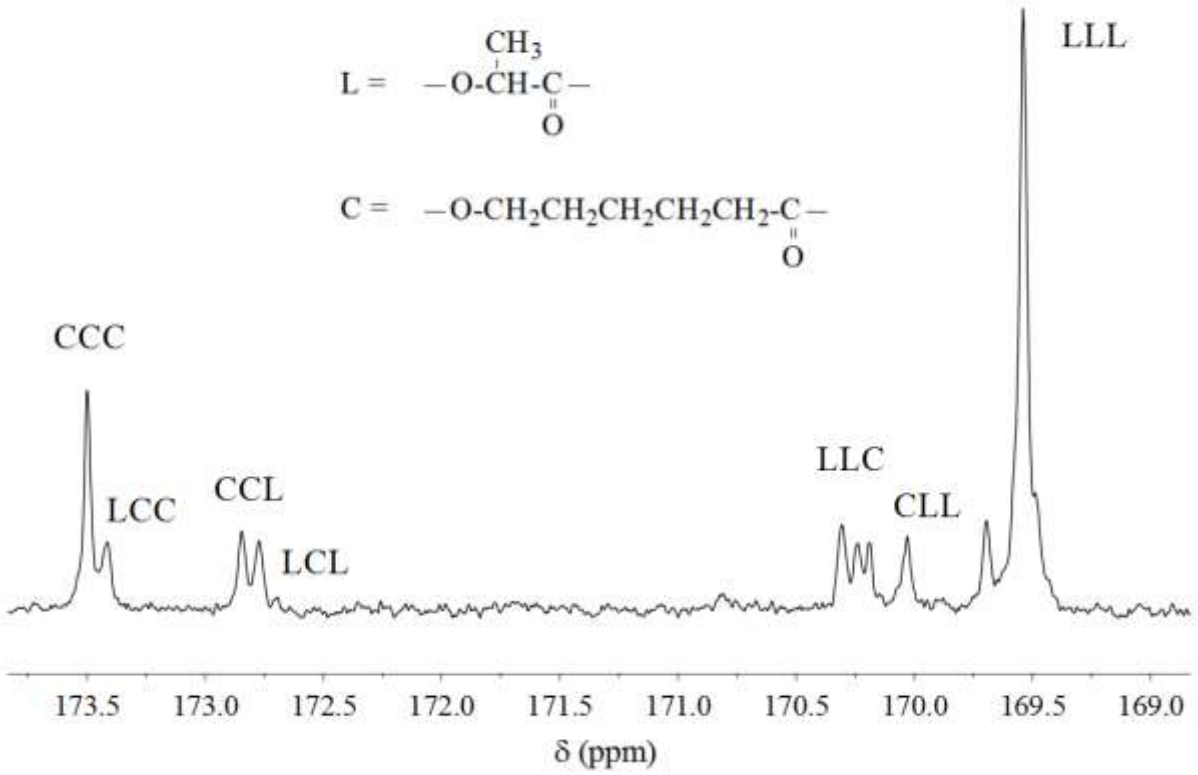


**Fig. 4** 100 MHz $^{13}$C-NMR spectrum (expanded C=O carbon region) of the PLLCL 50:50 copolymer recorded in $CDCl_3$ as solvent.

Thermal analysis by DSC showed the PLLCL copolymer to be completely amorphous with no observed cold crystallization $T_c$ or crystalline melting $T_m$ transitions and only a broad glass transition $T_g$ centered around -13 ºC. This amorphous nature was as expected from its near-equimolar 51:49 mol% composition. Together with its low $T_g$ and only moderate molecular weight, this amorphous morphology gave the copolymer the appropriate level of chain mobility for which it was purpose-designed as a compatibilizer. This $T_g$ and other properties of the PLLCL copolymer are compared with those of the PLL and TPU in Table 1.

**Table 1** PLL, TPU and PLLCL molecular weights, temperature transitions and initial degradation temperatures from GPC, DSC and TGA respectively

| Blend Component | GPC | | | DSC [b] | | | TGA |
|---|---|---|---|---|---|---|---|
| | $M_n$ $\times 10^{-4}$ | $M_w$ $\times 10^{-4}$ | *PDI* [a] | $T_g$ [c] (°C) | $T_c$ [c] (°C) | $T_m$ [c] (°C) | $T_d$ [e] (°C) |
| PLL | 15.2 | 25.5 | 1.68 | 59 | 127 | 153 | 290 |
| TPU | 12.8 | 26.2 | 2.05 | -18 [d] | – | – | 250 |
| PLLCL | 2.43 | 4.40 | 1.81 | -13 | – | – | 230 |

[a] *PDI* = polydispersity index = $M_w/M_n$ (where $M_w$ and $M_n$ have units of g/mol)
[b] DSC data obtained from 2nd heating scan after cooling from the melt at 10 °C/min
[c] Values given are the $T_g$ (mid-point), $T_c$ (minimum) and $T_m$ (maximum) temperatures
[d] $T_g$ determined by dynamic mechanical analysis (DMA)
[e] $T_d$ values are the initial weight loss temperatures from the TGA curves

## Polymer Blending

Polymer blends were formulated with PLL as the main component, TPU as a toughening agent and PLLCL as a compatibilizer. Based on a PLL content of 90 parts by weight (pbw), both 2- and 3-component blends were initially prepared with TPU and/or PLLCL contents ranging from 0-50 pbw. However, it soon became evident from the torque values observed during melt mixing that the upper limit of the TPU was 20 pbw, above which the melt

viscosity at 190-195 ºC became too high. This could be offset to a certain extent by the addition of the PLLCL copolymer as a plasticizer but, as the PLLCL content increased above 20 pbw, the *MFI* decreased rapidly until it became too low and the mechanical properties of hot-pressed films became severely weakened. Consequently, the primary objective was to find the blend composition which gave the best combination of melt viscosity, processability and overall (not only mechanical) film properties.

## Blend Properties

Even though blends containing up to 20 pbw TPU and/or PLLCL were processable in terms of melt mixing and hot pressing into films, it was found that the best overall film properties were obtained at the 10 pbw level for both the TPU and PLLCL. Therefore, although other compositions were studied, it is only the PLL/TPU/PLLCL 90/10/10 3-component blend which is described in this paper. The PLL/TPU 90/10 and PLL/PLLCL 90/10 2-component blends are also described in order to observe and compare the separate effects of the TPU and PLLCL. The various film properties studied, as discussed in the following sections, are summarized and compared in Table 2 for PLL, PLL/TPU 90/10, PLL/PLLCL 90/10 and PLL/TPU/PLLCL 90/10/10.

**Table 2** Comparison of the average values of the various properties of the PLL, PLL/TPU, PLL/PLLCL and PLL/TPU/PLLCL melt blends and hot-pressed films

| Property | PLL | PLL/TPU 90/10 | PLL/PLLCL 90/10 | PLL/TPU/PLLCL 90/10/10 |
|---|---|---|---|---|
| MELT BLENDS | | | | |
| Glass transition, $T_g$ (°C) [a] | 59 | 57 | 47 | 52 |
| Crystallization, $T_c$ (°C) [a] | 127 | 122 | 121 | 121 |
| Melting point, $T_m$ (°C) [a] | 153 | 150 | 147 | 151 |
| Crystallinity (%) [b] | 33 | 5 | 13 | 8 |
| Melt flow index (g/10 min) [c] | 6.42 | 3.75 | – [d] | 8.10 |

| | | | | |
|---|---|---|---|---|
| HOT-PRESSED FILMS [e] | | | | |
| Tensile strength (MPa) [f] | 38 | 26 | 25 | 28 |
| Strain at break (%) | 3 | 110 | 2 | 18 |
| Toughness ($J/mm^3$) [g] | | | | |
| Light transmittance (%) | 90 | 3 | 86 | 18 |
| *WVTR* ($g.mil/m^2.day$) [h] | 220.5 | 233.1 | 731.5 | 777.0 |
| *OTR* ($cm^3.mil/m^2.day.atm$) [h] | 445.9 | 452.9 | 802.9 | 961.8 |

[a] From DSC 2nd heating scans after cooling from the melt at 10 °C/min
[b] Initial % crystallinity ($\propto \Delta H_m - \Delta H_c$) from DSC 2nd heating scans ($\Delta H_m^* = 93.7$ J/g)
[c] Measured at 190 °C (load 2.16 kg; bore diameter 2.1 mm)
[d] Melt viscosity too low to produce a continuous extrudate at 190 °C
[e] Film thickness in the range of 150-200 μm
[f] Taken as the stress at break
[g] Calculated from the area under the stress-strain curve up to 10 % strain
[h] Normalized to a film thickness of 1 mil (1 mil = 25.4 μm)

## Thermal and Melt Flow Properties

From the DSC heating curves in Figs. 5 and 6 together with the data in Table 2, the presence of the immiscible TPU in the PLL/TPU 90/10 blend does not appear to have much effect on the PLL's temperature transitions. In contrast, the presence of the partially miscible PLLCL in the PLL/PLLCL 90/10 blend did significantly lower the PLL's $T_g$ by about 12 ºC due to its plasticizing effect. Interestingly, when the TPU and PLLCL were both present in the PLL/TPU/PLLCL 90/10/10 blend, the plasticizing effect of the PLLCL was reduced which could have been due to its partial association with the TPU domains. This possibility will be discussed in more detail later. It is also significant to note from the DSC cooling curves in Fig. 7 that the PLL and 2- and 3-component blends were all slow to crystallize from the melt at a cooling rate of 10 °C/min. Instead, most of the crystallization that occurred manifested itself as pre-melt crystallization during the 2nd heating scans, as shown in Figs. 5 and 6.

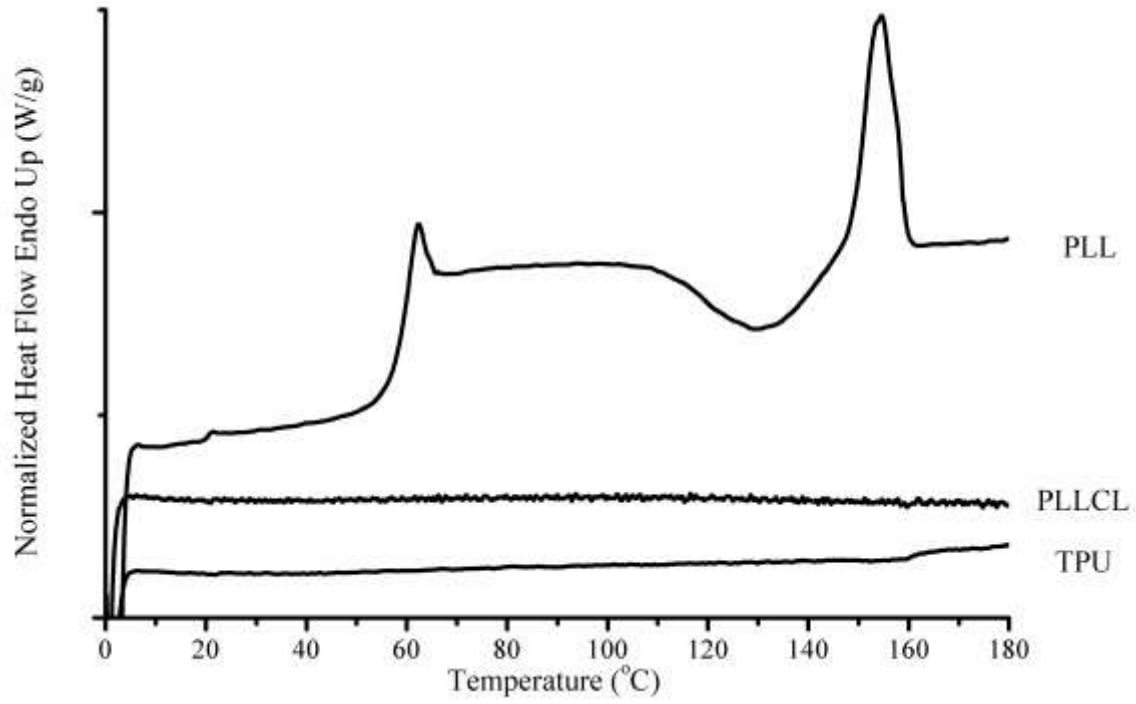


**Fig. 5** DSC heating curves of the PLL, TPU and PLLCL blend components (2nd heating scans, heating rate = 10 °C/min)

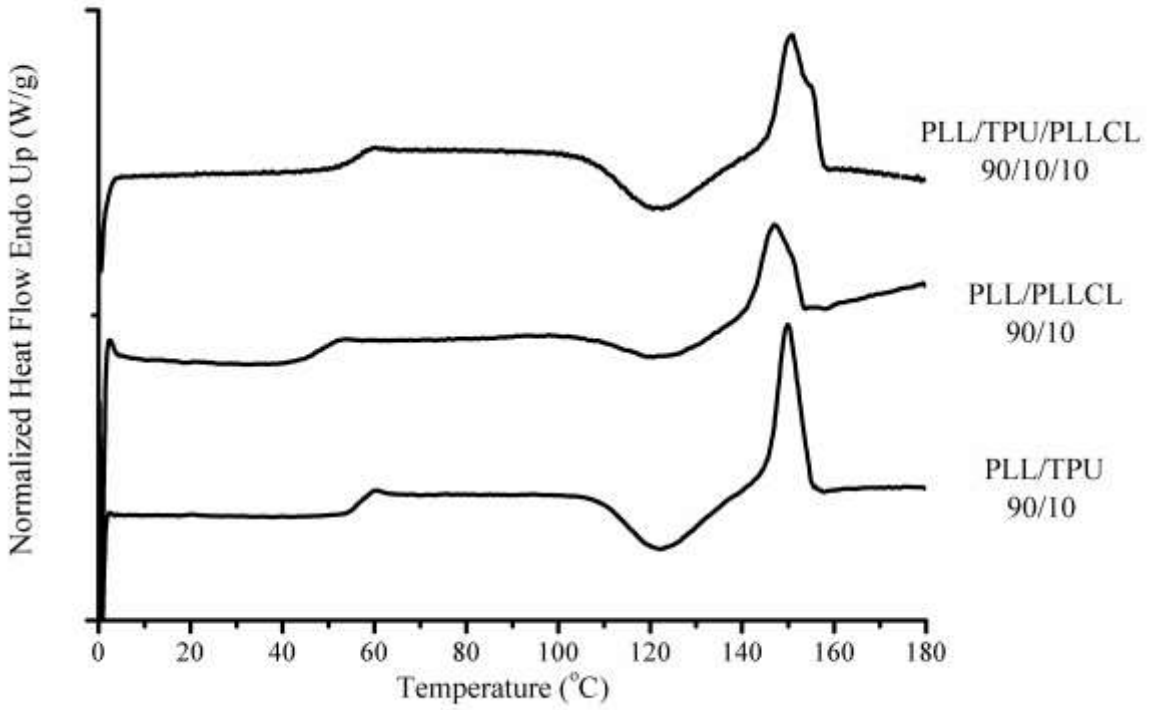


**Fig. 6** DSC heating curves of the PLL/TPU 90/10, PLL/PLLCL 90/10 and PLL/TPU/PLLCL 90/10/10 blends (2nd heating scans, heating rate = 10 °C/min)

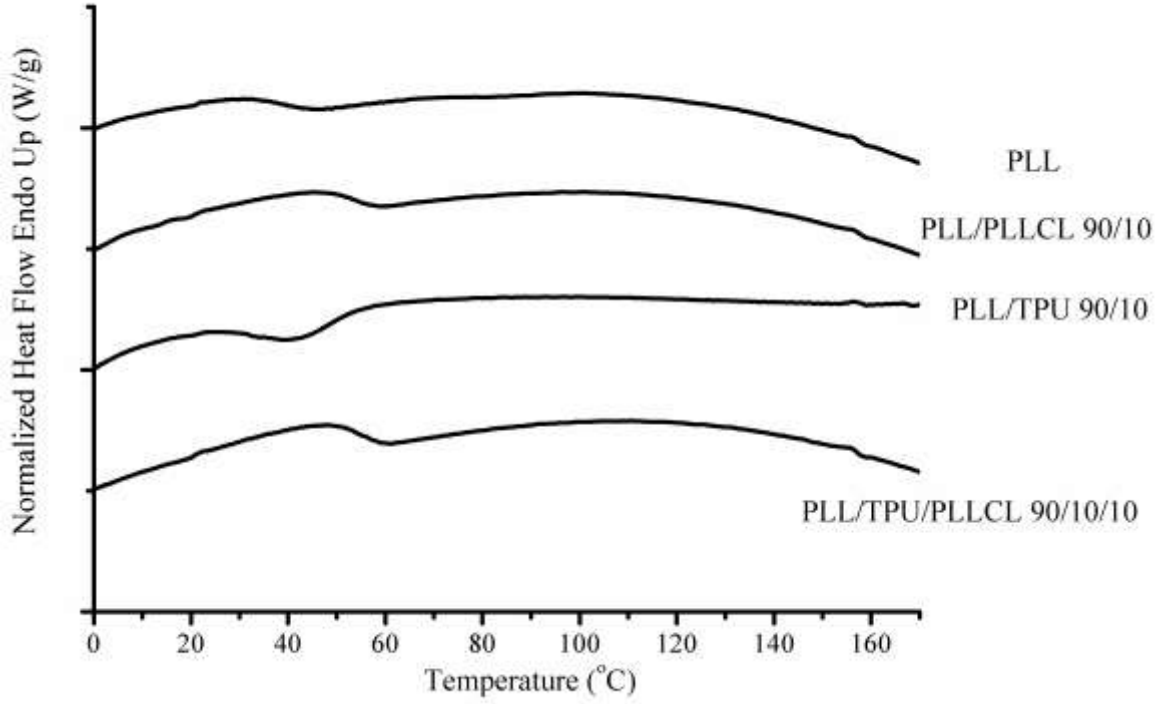


**Fig. 7** DSC cooling curves of PLL and the PLL/TPU 90/10, PLL/PLLCL 90/10 and PLL/TPU/PLLCL 90/10/10 blends (cooling rate = 10 °C/min)

Regarding the melt flow index data (*MFI*) in Table 2, the TPU and PLLCL have opposite effects on the PLL. Whereas TPU decreases the *MFI* (increases the melt viscosity) due to its hydrogen-bonded hard segments, PLLCL increases the *MFI* by plasticization. It is therefore significant to note in Table 2 that the *MFI* of the PLL/TPU/PLLCL 90/10/10 blend is higher than that of PLL. This indicates that, at the same 10 pbw level, the plasticizing effect of the PLLCL outweighed the stiffening effect of the TPU.

**Tensile Properties of Thin Films**

Typical stress-strain curves and derived parameters from tensile testing of the thin films are shown in Fig. 8 and Table 2. The main points to note are:

- The curves for PLL (a) and TPU (b) emphasize the fact that they are fundamentally different materials. Whereas PLL is a strong but brittle material with a strain at break of less than 5 %, TPU is a weak elastomeric material with a strain at break (not shown in Fig. 8) of more than 500 %.
- Curve (c) for the PLL/TPU 90/10 blend appears to be a combination of (a) and (b) suggesting that, although the TPU is able to toughen the PLL, there is limited interfacial adhesion between the two. The strain at break (also not shown in Fig. 8) was approximately 110 %.
- Curve (d) for the PLL/PLLCL 90/10 blend shows that addition of the PLLCL copolymer not only plasticizes the PLL but also weakens it considerably.
- When both the TPU and PLLCL are added in the PLL/TPU/PLLCL 90/10/10 blend, the result is a material which shows a stress-strain curve (e) intermediate in shape between those of PLL and PLL/TPU. The appearance of curve (e) as a much smoother and more continuous version of curve (c) suggests that the PLLCL is able to link the PLL matrix and the TPU domains together so that their responses to the applied stress overlap.

The toughening effect of TPU on PLL can be explained in terms of the dispersed TPU domains inducing deformation mechanisms which help to dissipate the applied strain energy, thereby avoiding the sudden brittle failure, as shown in curve (a), characteristic of PLL alone. However, the fact that the PLL/TPU 90/10 blend in curve (c) still shows a partial sudden failure between 2-5 % strain before levelling out suggests that the blend is acting partly like a physical mixture. This contrasts with curve (e) for the PLL/TPU/PLLCL 90/10/10 blend in which this sudden partial failure is eliminated resulting in a much smoother transition to plastic flow beyond the yield point. While this is not conclusive evidence in itself, it does at

least provide some qualitative support for the view that the PLLCL has been able to improve the level of PLL-TPU interaction at the interfaces between the two phases.

Although various techniques can point towards increased interfacial interaction in TPU-toughened blends, an improvement or at least a significant change in mechanical properties often provides the clearest evidence. A good example of this is the recent paper describing poly(3-hydroxybutyrate-*co*-3-hydroxyvalerate)/TPU blends in which tensile test data is supported by SEM images [37].

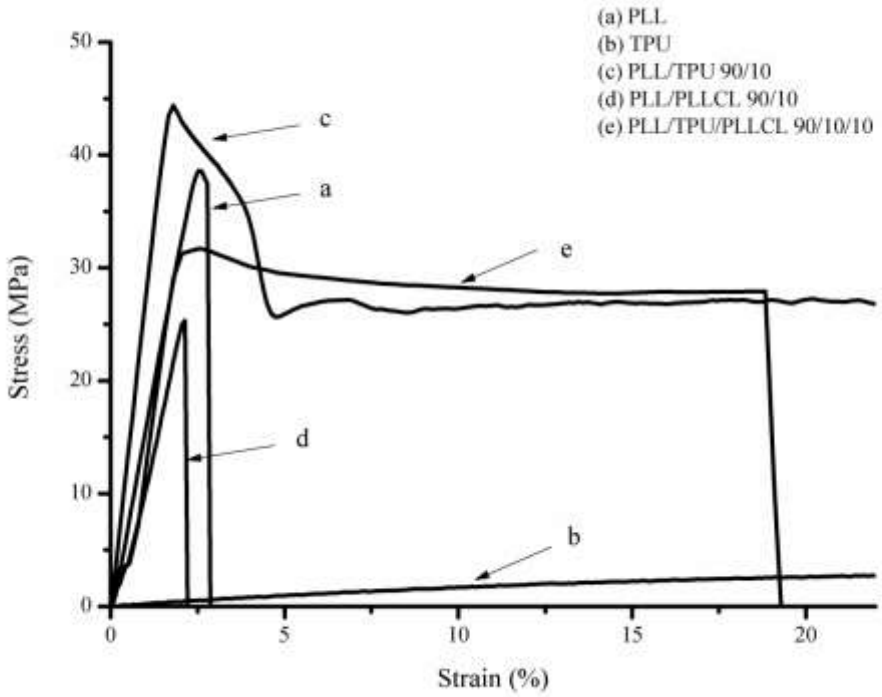


**Fig. 8** Stress-strain curves of thin films of the PLL, TPU and the 2- and 3-component blends. (Each curve is a typical example from tests carried out on a minimum of 5 test specimens.)

## Optical Clarity

The optical clarities of the thin films in terms of their light transmittance (%) are compared in Table 2. Whereas the PLL and PLL/PLLCL 90/10 films were essentially transparent with light transmittance values of around 90 %, the PLL/TPU 90/10 film was white and opaque with only 3 % transmittance. The fact that only 10 % pbw of TPU could transform the

otherwise transparent PLL into an opaque material is a consequence of the immiscibility of PLL/TPU leading to a phase-separated morphology in which the TPU domains are dispersed throughout the PLL matrix.

However, when the PLLCL copolymer was added in the PLL/TPU/PLLCL 90/10/10 blend, the level of opaqueness noticeably decreased to give a light transmittance of 18 %. This suggests a decrease in the average size and/or the size distribution of the dispersed TPU domains which reduces inherent light scattering from within the blend. When considered alongside the previous tensile results, this is a further indication that the PLLCL was able to increase the level of PLL/TPU interaction.

**Water Vapor and Oxygen Transmission Rates**

The water vapor transmission rates (*WVTR*) and oxygen transmission rates (*OTR*) for the thin films are compared in Table 2. The results show that, whereas 10 pbw of TPU had relatively little effect on the *WVTR* and *OTR* of PLL, 10 pbw of the PLLCL copolymer gave rise to significant increases in both the *WVTR* and the *OTR*. These increases are most likely due to the plasticizing effect of the PLLCL on the PLL rather than its chemical structure. Plasticization by the PLLCL decreases the $T_g$ and the % crystallinity of the PLL matrix and, in doing so, increases the amount of free volume between the chains through which water and oxygen molecules can pass.

Therefore, it must be concluded from these results that neither TPU nor PLLCL can improve the inferior water and oxygen barrier properties of PLL previously mentioned in the 'Introduction' section. Although the focus of attention here has been more on processability and mechanical properties, gas barrier properties are also very important, especially for food and drug packaging. Higher *WVTR* and *OTR* values indicate reduced moisture and oxidative protection which may shorten the shelf life of a moisture and/or air-sensitive product. Thus,

as they stand, these *WVTR* and *OTR* values in Table 2 indicate that these materials would only be suitable for packaging products which are not particularly moisture or air-sensitive.

**Matrix Morphology**

The phase-separated matrix morphology of the TPU-containing films can be clearly seen in Fig. 9 from SEM images taken of cross-sectional fracture surfaces. The TPU domains appear to vary in size from about 0.5-5 μm in diameter. This size range is somewhat larger than the 0.1-1 μm range which is usually considered to be the optimum range for a rubbery polymer to be an effective toughening agent for PLL.

Of particular interest in Fig. 9 is the comparison between the PLL/TPU 90/10 and PLL/TPU/PLLCL 90/10/10 blends. At the lower magnification of x2,000, the PLL/TPU/PLLCL 90/10/10 blend appears to have fewer of the larger-sized TPU domains which would be consistent with the increase in its optical clarity. However, apart from this, it should be emphasized that these SEM images at the macroscopic level, visually interesting though they are, are unable to provide any conclusive evidence regarding the level of interfacial interaction at the microscopic level between the PLL and TPU phases.

| Fracture Surfaces | PLL | PLL/PLLCL 90/10 | PLL/TPU 90/10 | PLL/TPU/PLLCL 90/10/10 |
|---|---|---|---|---|
| Magnification x 2,000 |  | 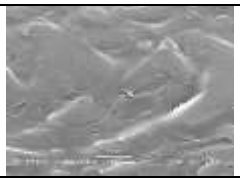 |  | 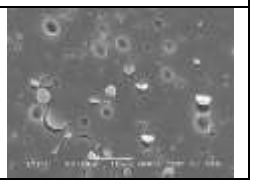 |
| Magnification x 10,000 |  |  | 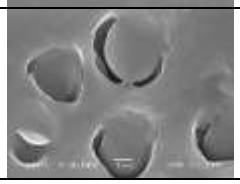 | 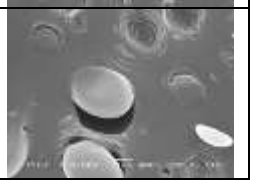 |

**Fig. 9** SEM images of cross-sectional fracture surfaces of the PLL and 2- and 3-component blends at different magnifications.

## Mechanism of Compatibilization

When considering a possible mechanism by which the PLLCL copolymer can act as a compatibilizer between the PLL and the TPU in order to improve the interfacial adhesion, a parallel can be drawn with the use of an A-B block copolymer to compatibilize its two parent but immiscible homopolymers. Previous work has suggested that the block copolymer, provided that it has sufficient molecular mobility, tends to migrate and become localized along the interfaces formed by its phase-separated homopolymers [38]. In doing so, the A and B blocks can interact with their respective homopolymers and form "bridges" across the interfaces. It was this rationale that provided the basis for the molecular design of the PLLCL copolymer used in this work. Even though it is not a block copolymer, the PLLCL is known to have a broad compositional distribution, is partly blocky, and its medium molecular weight, low $T_g$ and chain flexibility all combine to give it an appropriate balance between molecular mobility and melt viscosity.

This type of migration mechanism is visualized in Fig. 10 for the PLL/TPU/PLLCL system described here. Some of the PLLCL, especially the CL-rich fraction, migrates through the PLL matrix and becomes localized at the TPU domain interfaces where it can interact with the TPU's PCL soft segments. Conversely, the LL-rich fraction prefers to remain in closer contact with the PLL. Thus, the PLLCL distributes itself throughout the matrix according to its composition. In doing so, the CL-rich fraction acts a compatibilizer across the interface of some of the domains and it is this effect which improves the interfacial adhesion through secondary bonding forces such as dipole-dipole and methylene interactions.

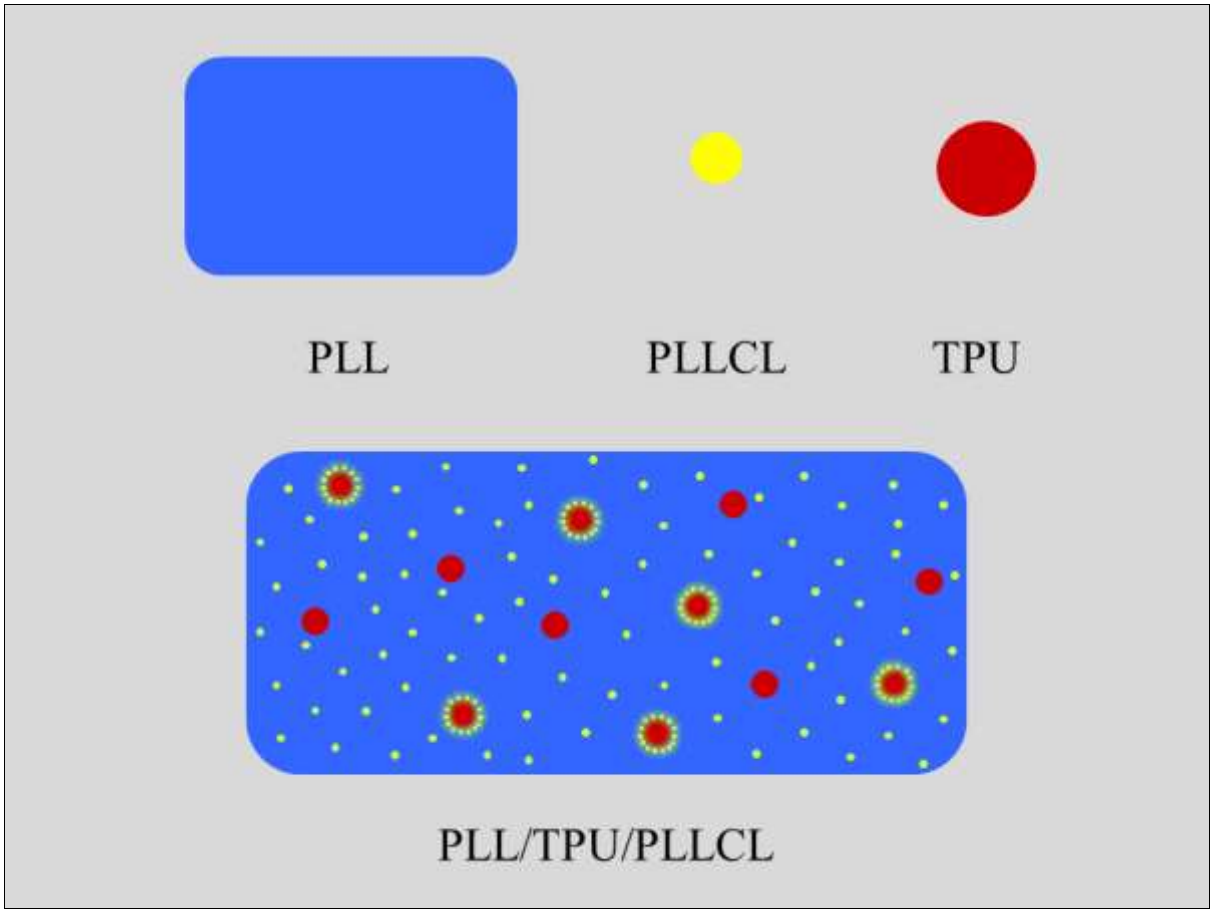


**Fig. 10** Visualization of the matrix morphology of the PLL/TPU/PLLCL blend showing the proposed compatibilizing effect of the PLLCL at the PLL/TPU interface.

## Biodegradability

The environmental biodegradation of PLL has been well-documented as being a two-stage bulk erosion process involving (1) simple hydrolysis of the ester groups to form low molecular weight oligomers and lactic acid followed by (2) microbial degradation of the fragmented residues by the microorganisms present to produce $CO_2$ and water [2-4, 39-41]. The first stage is a slow process during which hydration, hydrolysis and pore formation occur but with relatively little $CO_2$ production and weight loss. The majority of the weight loss occurs during the second stage when the microorganisms can start to digest the low molecular weight hydrolysis products. This two-stage process for PLL is different from those of many

other biodegradable polyesters which degrade by a single-stage surface erosion mechanism involving direct microbial attack with enzymatic degradation [42].

The biodegradation-time profiles for the PLL, PLL/TPU 90/10 and PLL/TPU/PLLCL 90/10/10 test samples alongside that of the cellulose reference are shown in Fig. 11 and the final average % biodegradation values after 90 days compared in Table 3. From these results, the main conclusions which can be drawn are as follows.

- The two-stage PLL profile in Fig. 11 is consistent with previous work. The first-stage induction period (as it is often referred to) of approximately 20 days, during which hydrolysis and molecular weight reduction occurred, produced minimal $CO_2$. This was then followed by a steady evolution of $CO_2$ during the second stage up to 78 % biodegradation after 90 days.
- The PLL/TPU 90/10 blend shows a similar 20-day induction period to PLL but is followed by a higher rate of degradation which can be attributed mainly to the blend's lower % crystallinity (Table 3). It is well known that hydrolysis occurs preferentially in the amorphous regions of the PLL matrix. The lower final % degradation of 67 % is probably due to the lower biodegradability of the TPU's hard segments.
- In marked contrast to the 2-component blends, the PLL/TPU/PLLCL 90/10/10 blend exhibits a single-stage biodegradation profile with no induction period and which is almost identical to that of the cellulose reference. This can only be explained in terms of the effect that the PLLCL copolymer has on the PLL matrix. Unlike PLL and TPU which are completely immiscible and phase-separated, PLL and PLLCL are partially miscible leading to a decrease in $T_g$ and an increase in free volume. Together with the reduced % crystallinity, this facilitates the diffusion of water through the matrix, thereby accelerating hydrolysis and pore formation. This is consistent with the previously mentioned increase in the *WVTR* (Table 2) when PLLCL is present in the blend.

- Finally, since the final % biodegradations relative to cellulose (Table 3) are all over 70 %, the test materials can all be classified as being "biodegradable plastics" according to the GreenPla JIS K 6953 (ISO 14855) Standard Test Method [43].

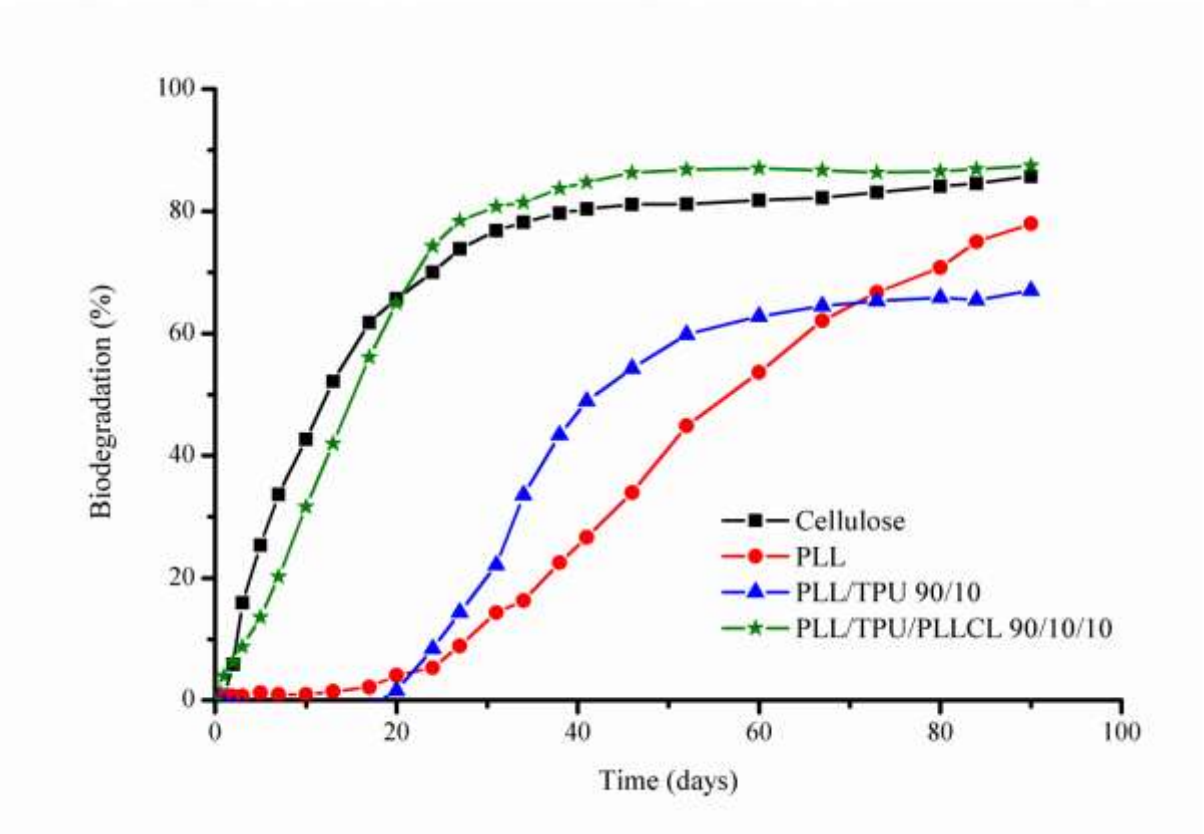


**Fig. 11** Biodegradation-time profiles for the PLL, PLL/TPU 90/10 and PLL/TPU/PLLCL 90/10/10 compared with cellulose as reference under controlled composting conditions.

**Table 3** Biodegradation (%) values after 90 days at 58 ± 2 °C of the cellulose (reference) and PLL, PLL/TPU 90/10 and PLL/TPU/PLLCL 90/10/10 test samples

| MATERIALS | Relevant Properties | | | Biodegradation (%) | |
|---|---|---|---|---|---|
| | Particle Size (μm) | $T_g$ (°C) | Crystallinity (%) | Average * value | Relative to cellulose |
| Cellulose | 20 | – | – | 85.7 | 100.0 |
| PLL | < 500 | 59 | 33 | 77.9 | 90.9 |
| PLL/TPU 90/10 | < 500 | 57 | 5 | 67.0 | 78.2 |
| PLL/TPU/PLLCL 90/10/10 | < 500 | 52 | 8 | 87.4 | 101.9 |

* Average values from 3 determinations; range of variation < 5 %

In summary, the appearance of an induction period depends on the time taken for the PLL molecular weight to be decreased to a level at which the residual chain fragments can be assimilated by the microorganisms present. This in turn depends on the rate at which water molecules can diffuse through the PLL matrix and hydrolyse the ester bonds leading to pore formation. Factors such as the PLL's initial molecular weight, % crystallinity, particle size, and its $T_g$ in relation to the biodegradation test temperature all have an effect.

Pore formation is obviously a key rate-determining step for $CO_2$ evolution. This helps to explain why blending with a second polymer usually accelerates PLL biodegradation. Previous work has suggested that domain boundaries and the interfacial area between the domains and the surrounding PLL matrix provide tracks along which water molecules can diffuse leading to hydrolysis, bulk erosion and eventually an interconnected pore structure [41, 44, 45]. However, what this present work has shown is that this also depends on the nature and distribution of the blend component. Even though the TPU was phase-separated from the PLL in clearly defined domains, it did not decrease the induction period. In contrast, addition of the more miscible PLLCL copolymer, which was distributed more uniformly throughout the PLL matrix as a whole, not only reduced but actually eliminated the induction period. Clearly, the PLLCL through its effect on water permeability has greatly increased the rates of hydrolysis and pore formation. However, this does not necessarily mean that the two-stage bulk erosion mechanism has changed, merely that the first stage has been accelerated to such an extent that it merges with the second.

## Conclusions

As stated at the end of the 'Introduction', the main objective of this work has been to improve the interfacial adhesion in a phase-separated PLL/PCL-based TPU melt blend by the addition

of a purpose-designed compatibilizer. The target application is biodegradable film packaging. Although TPU by itself can toughen PLL to a limited extent, it tends to have less desirable effects on other properties such as optical clarity and melt rheology. Therefore, the compatibilizer that was chosen – a medium molecular weight PLLCL 50:50 copolymer – was designed so that it would (a) have structural similarities with both the PLL matrix and the PCL soft segments of the TPU and (b) be amorphous with a low $T_g$ and low melt viscosity so that it could also act as a plasticizer for the PLL and a melt processing aid for the TPU.

When considered in combination, the results described here have demonstrated that the PLLCL copolymer can at least partially compatibilize the PLL and TPU by improving the interfacial interaction. This has been most clearly shown for the PLL/TPU/PLLCL blend by the shape of its stress-strain curve from tensile testing (Fig. 8e) and its light transmittance value (Table 2). It is proposed that this improvement is brought about by a localized concentration of CL-rich PLLCL molecules around the TPU domains which act as a "bridge" across the PLL/TPU interface. However, one disadvantage of PLL which has not been improved by the TPU and PLLCL is its inferior gas barrier properties. Instead, significant increases in both the *WVTR* and *OTR* (Table 2) highlight this as an area which requires further work.

Finally, the most surprising result came from biodegradability testing. Whereas PLL and the PLL/TPU blend each showed the expected induction period, the PLL/TPU/PLLCL blend did not. Instead, it showed a single-stage degradation profile very similar to that of the cellulose reference. For the addition of PLLCL to influence the biodegradability of the blend to such an extent was unexpected and is certainly one of the more significant findings to emerge from this work. When considered together with all the other results, it reinforces the view that this type of purpose-designed compatibilizer approach shows considerable potential

for not only improving the properties of PLL/TPU blends but also as a means of tailoring the properties, including biodegradability, to meet specific requirements.

**Acknowledgements** The authors wish to thank the Graduate School, Chiang Mai University, for the provision of a research grant for one of us (K.S.) and the National Research University Project under Thailand's Office of the Higher Education Commission for financial support.

## References

1. ASTM D5338-15, Standard Test Method for Determining Aerobic Biodegradation of Plastic Materials Under Controlled Composting Conditions, Incorporating Thermophilic Temperatures, ASTM International, West Conshohocken, PA, 2015
2. Auras RA, Lim L-T, Selke SEM, Tsuji H, Eds. (2010) Poly(lactic acid): Synthesis, Structures, Properties, Processing, and Applications, Wiley, Hoboken, USA
3. Ren J, Ed. (2010) Biodegradable Poly(Lactic Acid): Synthesis, Modification, Processing and Applications, Tsinghua University Press, Beijing, China
4. Piemonte V, Ed. (2014) Polylactic Acid: Synthesis, Properties and Applications, Nova Science, New York, USA
5. Endres H-J, Siebert-Raths A (2011) Engineering Biopolymers: Markets, Manufacturing, Properties and Applications, Hanser, Munich, Germany
6. Garlotta D (2001) J Polym Environ 9:63-84
7. Hamad K, Kaseem M, Yang HW, Deri F, Ko YG (2015) Express Polym Lett 9:435-455
8. Jamshidian M, Tehrany EA, Imran M, Jacquot M, Desobry S (2010) Compr Rev Food Sci Food Saf 9:552-571
9. Urquijo J, Guerrica-Echevarria G, Eguiazabal JI (2015) J Appl Polym Sci 132:42641. doi: 10.1002/app.42641
10. Ostafinska A, Fortelny I, Nevoralova M, Hodan J, Kredatusova J, Slouf M (2015) RSC Adv 5:98971-98982
11. López-Rodríguez N, López-Arraiza A, Meaurio E, Sarasua JR (2006) Polym Eng Sci 46:1299-1308
12. Zhang M, Thomas NL (2011) Adv Polym Technol 30:67-79

13. Yokohara T, Yamaguchi M (2008) Eur Polym J 44:677-685

14. Shibata M, Inoue Y, Miyoshi M (2006) Polymer 47:3557-3564

15. Jiang L, Wolcott MP, Zhang J (2006) Biomacromolecules 7:199-207

16. Kunthadong P, Molloy R, Worajittiphon P, Leejarkpai T, Kaabbuathong N, Punyodom W (2015) J Polym Environ 23:107-113

17. Singla RK, Maiti SN, Ghosha AK (2016) RSC Adv 6:14580-14588

18. Feng F, Ye L (2011) J Appl Polym Sci 119:2778-2783

19. Feng F, Zhao X, Ye L (2011) J Macromol Sci B 50:1500-1507

20. Lai S-M, Lan Y-C (2013) J Polym Res 20:140. doi: 10.1007/s10965-013-0140-6

21. Lai S-M, Wu W-L, Wang Y-J (2016) J Polym Res 23:99. doi: 10.1007/s10965-016-0993-6

22. Jing X, Mi HY, Salick MR, Cordie T, Crone WC, Peng X-F, Turng L-S (2014) J Cell Plast 50:361-379

23. Jaso V, Glenn G, Klamczynski A, Petrovic ZS (2015) Polym Test 47:1-3

24. Li Y, Shimizu H (2007) Macromol Biosci 7:921-928

25. Yuan Y, Ruckenstein E (1998) Polym Bull 40:485-490

26. Hyon S-H, Jamshidi K, Ikada Y (1997) Biomaterials 18:1503-1508

27. ASTM D1238-13, Standard Test Method for Melt Flow Rates of Thermoplastics by Extrusion Plastometer, ASTM International, West Conshohocken, USA, 2013

28. ASTM D882-02, Standard Test Method for Tensile Properties of Thin Plastic Sheeting, ASTM International, West Conshohocken, USA, 2002

29. ASTM F1249-13, Standard Test Method for Water Vapor Transmission Rate Through Plastic Film and Sheeting Using a Modulated Infrared Sensor, ASTM International, West Conshohocken, USA, 2013

30. ASTM D3985-05(2010)e1, Standard Test Method for Oxygen Gas Transmission Rate Through Plastic Film and Sheeting Using a Coulometric Sensor, ASTM International, West Conshohocken, USA, 2010

31. ISO 14855-1:2005, Determination of the ultimate aerobic biodegradability of plastic materials under controlled composting conditions – Method by analysis of evolved carbon dioxide – Part 1: General method, International Organization for Standardization, Geneva, Switzerland, 2005

32. Grijpma DW, Pennings AJ (1991) Polym Bull 25:335-341

33. Nalampang K, Molloy R, Punyodom W (2007) Polym Adv Technol 18:240-247

34. Kricheldorf HR, Kreiser I (1987) J Macromol Sci A 24:1345-1356

35. Kasperczyk J, Bero M (1991) Makromol Chem 192:1777-1787

36. Kasperczyk J, Bero M (1993) Makromol Chem 194:913-925

37. Martínez-Abad A, González-Ausejo J, Lagarón JM, Cabedo L (2016) Polym Degrad Stab 132:52-61

38. Spontak RJ, Patel NP, In: Hamley IW, Ed. (2004) Developments in Block Copolymer Science and Technology, Chap. 5, pp 159ff, Wiley, Chichester, UK

39. Lunt J (1998) Polym Degrad Stab 59:145-152

40. Rudeekit Y, Numnoi J, Tajan M, Chaiwutthinan P, Leejarkpai T (2008) J Metals Mater Minerals 18:83-87

41. Tsuji H (2008) Degradation of Poly(Lactide)-Based Biodegradable Materials, Nova Science, New York, USA

42. Tokiwa Y, Calabia BP (2007) J. Polym Environ 15:259-267

43. JIS K 6953 (ISO 14855), Determination of the ultimate aerobic biodegradability and disintegration of plastic materials under controlled composting conditions (Method by analysis of evolved carbon dioxide), Biodegradable Plastics Society, Japan, 2000

44. Tsuji H, Ishizaka T (2001) Int J Biol Macromol 29:83-89

45. Tsuji H, Ishizaka T (2001) Macromol Biosci 1:59-65